Novel systems for tailored neurotrophic factor release based on hydrogel and resorbable glass hollow fibers.

Novel systems for tailored neurotrophic factor release based on hydrogel and resorbable glass hollow fibers

G. Novajra[a,c], C. Tonda-Turo[b], C. Vitale-Brovarone[a], G. Ciardelli[b], S. Geuna[c], S. Raimondo[c]

[a] Department of Applied Science and Technology, Politecnico di Torino, Corso Duca degli Abruzzi 24, 10129 Torino, Italy

[b] Department of Mechanical and Aerospace Engineering, Politecnico di Torino, Corso Duca degli Abruzzi 24, 10129 Torino, Italy

[c] Department of Clinical and Biological Sciences and Cavalieri Ottolenghi Neuroscience Institute, University of Turin, Torino, Italy

Abstract

A novel system for the release of neurotrophic factor into a nerve guidance channel (NGC) based on resorbable phosphate glass hollow fibres (50P2O5-30CaO-9Na2O-3SiO2-3MgO-2.5K2O-2.5TiO2 mol%) in combination with a genipin-crosslinked agar/gelatin hydrogel (A/G_GP) is proposed.

No negative effects on the growth of Neonatal Olfactory Bulb Ensheathing Cell line (NOBEC) as well as on the expression of pro- and anti-apoptotic proteins was measured *in vitro* in the presence of fibre dissolution products in the culture medium. For the release studies, fluorescein isothiocyanate-dextran (FD-20), taken as growth factor model molecule, was solubilized in different media and introduced into the fibres lumen exploiting the capillary action. The fibres were filled with i) FD-20/ phosphate buffered saline (PBS) solution ii) FD-20/hydrogel solution before gelation iii)hydrogel before gelation, subsequently lyophilized and then filled with the FD-20/PBS solution. The different strategies used for the loading of the FD-20 into the fibres resulted in different release kinetics. A slower release was observed with the use of A/G_GP hydrogel. At last, poly(ε-caprolactone) (PCL) nerve guides containing the hollow fibres and the hydrogel have been fabricated.

Keywords
Glass hollow fibres; hydrogel; growth factor release; nerve guidance channel; *in vitro* test.

1. INTRODUCTION

The peripheral nerve axons can spontaneously regenerate after nerve injury thanks to the ability of the Schwann cells to promote a permissible environment for axonal growth [1]. In spite of this spontaneous regeneration, a complete recovery of nerve function after a severe lesion is unlikely to occur and clinical results have been, so far, unsatisfactory [2]. After peripheral nerve injuries, the capability of injured axons to regenerate and recover functional connections depends on the type of lesion and the distance over which the regenerating axons must grow to reinnervate their peripheral targets. After nerve crush, regeneration is usually successful, since the continuity of the endoneurial tubes is preserved [3].

In the case of more severe injuries, involving damages of the perineurium and endoneurium or the complete nerve transection, the spontaneous regeneration process is compromised and a surgical intervention becomes necessary [4]. For large nerve defects, in which direct suture of the two stumps (i.e. end-to-end suture) would generate excessive tension, the bridging of the gaps with an autologous nerve graft is currently considered the current gold standard [4,-5]. The use of a nerve guidance channel (NGC) sutured in between the two nerve stumps represents an alternative to autograft implantation, avoiding the additional surgical procedure needed for nerve graft harvesting. Moreover, NGC implies a less surgical trauma due to fewer epineurial sutures, the absence of any interference from the imperfectly aligned autograft fascicles, the minimization of fibrous scar tissue infiltration and the maximization of soluble factors accumulation [5].

Some NGCs are currently available on the market [4,6,7], but their use is limited to short nerve defects, up to about 3 cm [8]. For large nerve gaps, an inadequate formation of the fibrin cables between the two nerve stumps limits the migration of native SCs and the formation of Bands of Büngner, which are the trophic and topographical guidance structures for the regenerating axons growing from the proximal stump. Another important issue can be an insufficient neurotrophic support into the NGC [9]. For these reasons, there is a need to confer additional functionalities to the NGCs in order to improve the regeneration of longer nerve defects. A number of neurotrophic factors have been shown to stimulate axonal regeneration when placed in the lumen of the tube. These include the nerve growth factor (NGF) [10], fibroblast growth factor (FGF)

[11], vascular endothelial growth factor (VEGF) [12], insulin-like growth factor-I (IGF-I) [13] and a combination of the platelet-derived growth factor BB (PDGF-BB) and IGF-I [14]. Growth factors (GFs) are usually delivered via a carrier because of their limited activity *in vivo*; for instance, VEGF has a clearance half-life of less than 1 hour following injection *in vivo* [15]. Therefore, systems guaranteeing the stability and a controlled release of a GF are required in order to mimic the temporal presence of GFs in the biological environment.

In a previous study, Vitale-Brovarone *et al.* [16] showed that phosphate glass fibres are able to support glial and neuronal cell adhesion and to direct the growth of long axons, showing to be promising for the a promising creation of topographical guidance structures for cells during nerve regeneration.

Moreover phosphate glass hollow fibres could easily incorporate a liquid exploiting the capillary action and subsequently release it [17]. In this study, phosphate glass hollow fibres are proposed as a means for the incorporation and release of neurotrophic factors into a NGC. Fluorescein isothiocyanate-dextran (FD-20) is selected as a model molecule to study the release of biomolecules from the glass fibres. FD-20 is a fluorescent molecules having a Mw around 22 kDa and a Stokes radius of 33 Å (supplier's data) comparable to the dimensions of many relevant GFs in nerve regeneration (e.g., NGF VEGF, brain-derived neurotrophic factor - BDNF, glial cell-derived neurotrophic factor-GDNF, all having molecular weights in the range of 20–30 kDa as dimers) [18].

In order to tailor the release kinetics from the glass hollow fibres, an agar (A)/gelatin (G) hydrogel crosslinked with genipin (A/G_GP) is proposed as a filler for the hollow fibres. This hydrogel was previously described by Tonda-Turo *et al.* [19] as an injectable filler for NGCs.

The mild conditions for hydrogel preparation (low temperature and physiological pH) are advantageous for the incorporation of bioactive molecules avoiding their denaturation, while hydrogel microporosity allows an efficient biomolecule delivery.

Finally, a multifunctional NGC was fabricated filling a porous poly(ε-caprolactone) (PCL) guide with both glass hollow fibres and A/G_GP hydrogel.

2. MATERIALS AND METHODS

2.1 Hollow fibre drawing

Phosphate glass hollow fibres (glass composition $50P_2O_5$-30CaO-$9Na_2O$-$3SiO_2$-3MgO-$2.5K_2O$-

2.5TiO_2 mol %, Coded as $TiPS_{2.5}$ [20–21]) were drawn using an in-house developed drawingtower equipped with an online optical fibre diameter monitor, as previously described [16]. In brief, the precursors of the glass (Sigma-Aldrich) were melted in a 90Pt/10Rh %wt crucible in a furnace and cast into a pre-heated (below 440°C, which is the glass transition temperature) stainless steel mould, subsequently rotated around its longitudinal axis (3400 rpm) using an homemade rotational equipment (no load motor, 50W). A cylindrical glass hollow preform (outer and inner diameter, D_{po}= 11.3 mm and D_{pi}=6.5 mm, respectively 11.3 mm) was obtained and then annealed (410°C, 15 h). The preform was heated at 610 °C in the drawing tower causing the formation of a neck-down region with the creation of a thin fibre which was collected on a rotating drum. Acting on the preform feeding speed, v_p, and the fibre speed, v_f, it was possible to obtainn two type of fibres (coded as FA and FB) with different diameters (Table 1). The theoretical fibre outer (TD_{fo}) and inner (TD_{fi}) diameters were calculated imposing the mass conservation law and the retention of the outer to inner diameter ratio of the hollow preform (R= $D_{fo}/D_{fi} = D_{po}/D_{pi}$ = 1.74) using the following formulas:

(1) $TD_{fo} = D_{po}\sqrt{(v_p/v_f)}$

(2) $TD_{fi} = TD_{fo}/R$

The fibres were observed using an optical microscope and the outer and inner diameters (D_{fo} and D_{fi}) of the obtained fibres were measured on 20 fibre sections by image processing (Image J software).

2.2 Biological test with the fibre dissolution products

The effect of the fibre dissolution products was studied on Neonatal Olfactory Bulb Ensheathing Cell line (NOBEC), derived from primary cells dissociated from neonatal rat olfactory bulb and immortalized by retroviral transduction of SV40 large T antigen [22].

Two samples of hollow fibres (FB, 2 cm) were sterilized in an oven (180°C, 3 h), soaked in Dulbecco's Modified Eagle Medium (DMEM; Sigma-Aldrich) supplemented with 100 units ml^{-1} penicillin, 0.1 mg ml^{-1} streptomycin, 1 mM sodium pyruvate, 2 mM L-glutamine and 10% heat-inactivated fetal bovine serum (FBS; all from Invitrogen) at a (solution volume)/(fibre exposed

surface) ratio of 1 ml/cm^2 and stored at 37°C in a humidified atmosphere of 5% CO_2/air. Moreover, it was verified that the heat sterilization process (180°C, 3 h) do not interfere with the possibility of filling the hollow fibres.

At different time points (3, 14, 21 and 28 days) the medium was collected and the fibres were washed in distilled water, dried in an oven at 37°C and weighed. The weight loss percentage at the time point *i* was calculated using the following formula:

$$(3)\ \%WL_i = 100\ (W_0 - W_i)/W_0$$

where W_0 and W_i are, respectively, the sample weight at the beginning of the test and at the time point *i*.

The weight loss rate per unit area (WLR) was calculated dividing the final weight loss (WL) of the samples at the end of the test by the test duration t and by the exposed surface area A, which was approximated as the inner and outer lateral surface of an hollow cylinder of length L and inner and outer diameter equal to D_{fi} and D_{fo}:

$$(4)\ WLR = WL/(tA) = WL/\ [t\pi L\ (D_{fo} + D_{fi})]$$

In order to evaluate the dissolution products effects on cells, a proliferation cell curve was carried out with media collected after 14 and 28 days of fibre dissolution (sample code, respectively 14F, 28F). As control media, samples of culture medium without fibres were maintained in the same conditions of the fibre-containing samples and then collected after 14 and 28 days ("aged" media, ctrl14, ctrl28). For each test also "fresh" culture medium (ctrl) was used. The media (14F, 28F, ctrl14, ctrl28) were supplemented with 100 units ml^{-1} penicillin, 0.1 mg ml^{-1} streptomycin, 1 mM sodium pyruvate, 2 mM L-glutamine and 10% heat-inactivated fetal bovine serum (FBS; all from Invitrogen) before *in vitro* tests. About 2000 cells/cm^2 were cultured in a 12-well plate in the presence of 1 ml of the media containing the fibre dissolution products (14F) and the control media (ctrl, ctrl14). After 1, 3 and 5 days of incubation, the cells were washed with phosphate buffered saline (PBS; Invitrogen) and detached by incubation with 500 µl of trypsin (Sigma-Aldrich) for 5-10 min at 37°C. Complete medium was added to inactivate trypsin and then cells were counted using a Bürker's chamber. The study was carried out in triplicate and reported as mean value ± standard error of the mean.

About 27000 cells/cm^2 were cultured in a 12-well plate in the presence of 1 ml of the medium containing the fibre dissolution products (28F) and the control media (ctrl, ctrl28). After 3 days

of culture total proteins were extracted from 3 different wells by solubilizing cells in boiling Laemmli buffer (2.5% SDS and 0.125 M Tris-HCl pH 6.8), followed by 3 min at 100°C. Protein concentration was determined by the bicinchoninic acid assay (BCA) method, and equal amounts of proteins (denaturated at 100°C in 240 mM 2-mercapto ethanol and 18% glycerol) were separated on a 12% polyacrylamide gel, consisting of Acrylamide-bisacrylamide 12%; 0.375M Tris pH 8.8, 0.1% SDS, 0.1% ammonium persulfate and tetramethylethylenediamine (TEMED) 0.06%, to which was applied a voltage of 150 volts for approximately 2 hours. The protein gel was subjected to transfer on a nitrocellulose membrane and blocked for 1 h at 37 °C in 1X TBST (150 mM NaCl, 10 mM Tris-HCl (pH 7.4), and 0.1% Tween) plus 5% non-fat milk. The membranes were incubated overnight at 4 °C in primary antibodies: anti-Bcl-XL (Santa Cruz) diluted 1:500, anti-Bax (Santa Cruz) diluted 1:500 in TBST plus 1% non-fat milk. The next day, they were rinsed four times with TBST for 5 min each at room temperature and incubated for 1 h at room temperature with horseradish peroxidase-linked anti-mouse (1:10,000) secondary antibody (diluted in TBST plus 1% non-fat milk). Membranes were washed 4 times, 5 min each, with TBST at room temperature, and specific binding was detected by the enhanced chemiluminescence ECL system (Amersham Biosciences) using HyperfilmTM (Amersham Biosciences).

2.3 Hydrogel preparation

The genipin crosslinked agar/gelatin hydrogel (A/G_GP) was prepared as described elsewhere [19]. In brief, A (Sigma Aldrich) was dissolved in PBS at 90°C in an oven for 1 hour to obtain a 0.4 % (wt./vol.) solution. The solution was kept under magnetic stirring at 50°C for 30 minutes. G (type A from porcine skin, Sigma Aldrich) was added to obtain a A/G 20/80 wt./wt. solution 2% wt./vol., which was kept under magnetic stirring at 50°C for 30 minutes. Finally, GP was added to the A/G solution at a 2.5% wt./wt. amount with respect to the total amount of A and G. The resulting A/G_GP solution was kept under magnetic stirring at 50°C for 30 minutes and used as described in the next paragraphs.

2.4 Study of FD-20 release from the hollow fibres

Different release studies were carried out from the hollow fibres using FD-20 (Sigma Aldrich) as a model molecule. FD-20 was solubilized in PBS or was loaded into the A/G_GL hydrogel prior

to gelification and introduced into the fibres lumen exploiting the capillary action following different strategies. The different samples used for the release studies are summarised in Table 2. Different fibres and filling procedures were applied to evaluate their influence on biomolecules release.

For the first set of experiments, the influence of inner and outer fibre diameters and fibre length on FD-20 release was analysed. FA fibres of 2 cm and FB fibres with different length (1.5, 2 and 2.5 cm) were filled with a FD-20/PBS solution (10 mg/ml) exploiting the capillary action by soaking one of the fibre bundle extremities into the solution (sample codes, respectively, FA-2, FB-1.5, FB-2, FB-2.5).

For the second set of experiments, samples of FB fibres with a length of 2 cm were filled with FD-20-containing hydrogel - (sample code FB-2-H). The hydrogel were prepared as described in paragraph 2.3 and FD-20 was added into the A/GL_GP solution (10 mg/ml) prior to gelification. The fibres were then filled with the FD-20/hydrogel solution before gelification exploiting the capillary action as described before. Fibres were kept at room temperature until hydrogel gelification occurred and then stored at 4°C until they were used for the release study.

For the last set of experiments, FB fibres with a length of 2 cm were filled with the A/G_GP solution before gelification, kept at room temperature until hydrogel gelification occurred, frozen at -20°C for 24 hours and then lyophilized using a SCANVAC Coolsafe 5P freeze dryer. Finally, the cavity of the fibres, containing a porous matrix of lyophilized hydrogel, was filled with a FD-20/PBS solution (10 mg/ml) exploiting the capillary action (sample code FB-2-LH). The sample morphology resulting from different filling procedures (FA-2, FB-1.5, FB-2, FB-2.5; FB-2-H, FB-2-LH) was observed using an optical microscope (Nikon Optishot Microscope).

To study the FD-20 release profile of the different FD-20-containing fibres, fibres of each type (FA-2, FB-1.5, FB-2, FB-2.5, FB-2-H and FB-2-LH, table 2) were soaked in PBS ((solution volume)/(fibre exposed surface) of 1 ml/cm^2) into a flask and stored at 37°C. 5 ml of medium was taken at different time points until no further change in FD-20 concentration was observed (1, 5, 22, 24, 48 h for FA-2, FB-1.5, FB-2 and FB-2.5; 1, 5, 24, 31, 48, 72, 144, 168, 192 h for FB-2-H; 1, 5, 24, 31, 48, 72, 144 h for FB-2-LH). The medium was analysed using UV-Vis spectrophotometer (Cary 500 Varian) for absorbance measurement (FD-20 main absorbance peak at 490 nm) and then replaced into the flask. The glass dissolution products derived from the fibre dissolution in PBS caused the presence of a peak at about 250 nm in the UV-Vis absorption spectrum showing increasing amplitude with time, which interfere with the FD-20 peak. For this

reason, the UV-Vis spectrophotometer calibration curves were derived at each time points using FD-20/PBS solutions (6.25, 12.5 25, 50, 100 µg/ml) containing samples of glass fibres, prepared and stored in the same conditions used for the samples of the release test ((solution volume)/(fibre exposed surface) of 1ml/cm^2, stored at 37°C). Moreover, a refresh of the medium was carried out twice a week for the samples requiring longer soaking time (FB-2-H and FB-2-LH).

For each sample, the FD-20 release percentage at the time point *i* was calculated using the following formula:

(5) $\%Release_i = 100C_i/C_{max}$,where C_{max} and C_i are, respectively, the maximum FD-20 concentration measured at the end of the test (i.e. when all FD-20 had been released) and the FD-20 concentration measured at the time point i. For the measures performed after medium refresh, Ci was calculated as the sum of the concentration measured at the time point i and those measured before the refresh. The release percentage is reported as mean value and standard deviation for each type of sample.

The release profile curves were interpolated on the basis of the semi-empirical power law

(6) $M_i/M_\infty = Kt^n$

and the Weibull function:

(7) $M_i/M_\infty = 1-exp(-at^b)$,

in which M_i and M_∞ are, respectively, the amount of FD-20 released at time *t* and at infinite time, *k* is the kinetic constant. The n parameter depends on the geometry of the system and on the drug release mechanisms (equation 6), while *a* and *b* are constants (equation 7) [23,-24].

In terms of concentration and % release, equation 6 and 7 can be rewritten as:

(8) $C_i/C_{max}=\%Release_i /100 = Kt^n$,

(9) $C_i/C_{max}=\% Release_i /100 =1-exp(-at^b)$.

Since the semi-empirical power law is a short time approximation ($M_i/M_\infty<0.6$) [23], the interpolation with equation 8 was limited to the first 60% of the release curve, while equation 9 was used for the entire release curve.

2.5 Feasibility and morphological evaluation of multifunctional nerve guidance channel

Poly(ε-caprolactone) (PCL) porous tubes were obtained as described elsewhere [25]. Briefly, a 3 mm stainless steel rotating mandrel (diameter 3 mm) was dipped into PCL / polyethylene oxide (PCL/PEO, 60/40 wt./wt.) solution, left air-dried for 12 hours and, then, immersed in PBS for 2 days to remove PEO and obtain a porous wall structure. The tubes were cut to obtain samples of 1.5 cm of length. A bundle of hollow fibres (FB, 1.5 cm length, about 120 mg) filled with the hydrogel (as described at paragraph 2.4) was inserted into the PCL tube. Finally, the hydrogel was injected before gelification with a pipette in order to completely fill the tube lumen. The PCL tube/glass hollow fibres system was kept at ambient temperature until hydrogel gelification. The morphology of the resulting guide was analysed using a scanning electron microscope (SEM; Quanta Inspect 200LV, Fei Company, The Netherlands). For the analysis the guide was embedded in epoxy resin (Epofix, Struers) and cut by a diamond disc saw (Struers Accutom 5, cut-off wheel 330CA) to obtain a section. The guide was also analysed by X-ray absorption microtomography (μCT, SkyScan 1174v2, SkyScan N.V., Kontich, Belgium) to obtain a three-dimensional image of the structure of the guide (50kV, 880 μA, exposure time 1900 s, pixel size 6.5 μm).

3. RESULTS AND DISCUSSION

3.1 Hollow fibres

The inner and outer fibre diameters of the hollow glass fibres (D_{fi} and D_{fo}) were 69 ± 5 μm and 121 ± 4 μm for FA and 94 ± 3 and 167 ±4 μm for FB, respectively. These values are in agreement with the theoretical ones (Table 3).

3.2 Biological test with the fibre dissolution products

Results of dissolution study for the hollow fibres (FB, 2 cm) soaked in culture medium are reported in Fig.~~ure~~ 1. A weight loss percentage (%WL) of 14% ± 4% after 28 days (Fig. 1), corresponding to a weight loss rate per unit area (WLR) of $1.6 \cdot 10^{-8} \pm 0.5 \cdot 10^{-8}$ g cm^{-2} min^{-1}~~.~~ was measured. The values obtained are of the same order of magnitude, but slightly lower, than those

measured in a previous study on slices of $TiPS_{2.5}$ glass soaked in bi-distilled water, ($8 \cdot 10^{-8} \pm 1.2 \cdot 10^{-8}$ g cm^{-2} min^{-1}). The slower dissolution of $TiPS_{2.5}$ glass in culture medium probably due to the presence of serum proteins and of some ions in solution, like Ca^{2+}, which are known to hinder the glass dissolution [21,26].

The media containing the fibre dissolution products were used for *in vitro* test to study their influence on NOBEC cells. The proliferation curves of NOBEC cells incubated with media containing the fiber dissolution products after 14 days of dissolution (14F) and the control media (ctrl, ctrl14) are reported in Fig. 2.

No significant differences between all experimental groups (ctrl, ctrl14, 14F) were observed after 1, 3 and 5 days of culture,showing that dissolution products did not influence cell survival and proliferation.

In order to verify the absence of a cytotoxic effect of dissolution products, ctrl, ctrl28 and 28F samples were analyzed by Western blot for apoptotic proteins expression after 3 days of culture. Bax, a cytosolic protein that plays a pro-apoptotic role, and Bcl-xl, a pro-survival protein, have the same expression in ctrl, ctrl28 and 28F (Fig. 3).

3.3 Study of FD-20 release from the hollow fibres

In this study, the use of phosphate glass hollow fibres for the release of FD-20, as model molecule for growth factors such as NGF, VEGF, BDNF, GDNF was studied. The possibility of tailoring the FD-20 release kinetics was investigated acting on different strategies for molecule encapsulation (paragraph 2.4, table 2).

As previously demonstrated, phosphate glass hollow fibres can be easily and quickly filled with a liquid solution exploiting the capillary action by soaking one of the fibre extremities into the solution [17]. Using this procedure, the FD-20/PBS solution was used to fill the glass hollow fibres (Fig. 4a). The same procedure was applied to fill the hollow glass fibres with a FD-20/hydrogel solution before gelification (Fig. 4b). Another approach consisted in filling the fibre with the hydrogel alone followed by a lyophilisation to produce a porous hydrogel matrix into the fibre lumen (Fig. 4c). The presence of the lyophilized hydrogel did not hinder filling these fibres with a FD-20/PBS solution by capillary action later on (Fig. 4d).

All the described strategies were successful in filling the fibres, as desired.

The FD-20 release from hollow fibres was studied by varying different parameters, such as fibre

size and method for incorporation of FD-20 into the fibre lumen.

Fig. 5 shows the FD-20 release percentage from fibres filled with FD-20/PBS (FA-2, FB-1.5, FB-2, FB-2.5). All the fibre types released more than 95% of FD-20 in the first 24h. Since the release of FD-20 is associated to a diffusion process of the molecule out of the fibres from the open ends, it would be expected, by the same D_{fi} (FB-1.5,FB-2, FB-2.5), a slower release for fibres with greater length L, as observed by Hong *et al.* [27]. Kosmidis *et al.* [24] observed that the release kinetic is connected to the specific leak surface, that is the ratio between the area available for the molecule release ($1/4 \cdot \pi D_{fi}^2$ in this case), and the volume containning the molecule (i.e. $1/4 \cdot \pi D_{fi}^2 \cdot L$ in this case), with faster release for a higher specific leak surface. Thus, longer hollow fibres would show lower specific leak surface (i.e. $1/L$ in this case) and then slower release kinetics. However, even if the mean values show this trend at 1 and 5 h (FB-1.5 > FB-2 > FB-2.5), they did not present a statistically significant difference (one way ANOVA, $p<0.05$).

Moreover, also different D_{fi} (FA-2 and FB-2) did not influenced the release kinetics in a statistically significant manner.

Since fibre size did not influence the release of FD-20, the sample coded as FB-2 (table 2) having Dfi = 94 ± 3, Dfo= 167 ± 4 and length of 2 cm was selected to compare the FD-20 release using different filling procedures.

Fig. 6 shows the release profile from fibres of identical size (inner diameter and length) loaded with FD-20 using different strategies (FB-2, FB-2-H, FB-2-LH). The use of A/G_GP hydrogel both in the hydrated and lyophilized state as hollow fibre filler alloweda slower release compared to fibres filled with the FD-20/PBS solution. The fibres filled with FD-20/hydrogel (FB-2-H) showed a complete release after 168 h, while those containning the lyophilized hydrogel and filled with FD-20/PBS solution (FB-2-LH) showed a complete release already after 72 h.

The solubilisation of the FD-20 into the A/G_GP solution prior to gelification (FB-2-H) allowed FD-20 encapsulation inside the hydrogel obtaining a prolonged release; an initial burst release (36±4%) from the surface of the hydrogel is followed by a sustained release stage of FD-20 contained into the hydrogel mesh.

On the other hand, FB-2-LH samples showed a significantly higher burst release (52±6%) compared to FB-2-H because of the presence of the FD-20/PBS solution filling the interconnected macropores of the lyophilized hydrogel. Consequently, the leakage of FD-20 from the fibres is made easier. The prolonged release observed after the initial burst release can

be ascribed to the penetration of the FD-20 inside the hydrogel after PBS absorption during hydrogel swelling. About 45% of FD-20 was entrapped into the lyophilized hydrogels and slowly released afterwards.

In order to have a better insight into the release mechanism associated to the different FD-20-loaded hollow fibres, the interpolation of all the release data was carried out on the basis of the semi-empirical power law for the initial 60% of the release curve and the Weibull function (equation 6 and 7). The regression curve of FB-2, FB-H and FB-2-HL are represented in Fig. 7a-b, in which the values of the parameters *n*, *a* and *b* are also reported. The regression curves of FB-1.5 and FB-2.5 are not reported since they were very similar to those of FB-2 and would overlap in the graph. The value of n in the semi-empirical power law is related to the geometry of the system and the release mechanism. For example, in thin film geometries, n is 0.5 for pure Fickian diffusion and 1 for swelling-controlled release mechanism [28]. Papadopoulou *et al.* [23] interpolateed the drug release from several available data using the power law (initial 60% of release) and the Weibull function (entire release data) and then performed a linear regression on the obtained *n* and *b* values. They showed that exponent *b* of the Weibull function is linearly related to *n*. As observed in Fig. 8 the obtained value of *n* and *b* for the different FD-20 releasing hollow fibres are in accordance with the linear regression curve (dotted line) obtained by Papadopoulou *et al.* [23]. They also found that the value of *b* is related to the mechanism of drug transport. For the diffusion in normal Euclidian space, they found *b* values in the range 0.69-0.75, which is very close to that found in this work for the release from hollow fibres filled with FD-20/PBS (0.65 ± 0.07 to 0.82 ± 0.12). The lower values of *b* found for the other samples (0.54 ±0.08 for FB-2-H and of 0.49 ± 0.04 for FB-2-LH) can be ascribed to the presence of the hydrogel. In fact, a decrease of *b* reflects an increase of the disorder of the medium in which the Fickian diffusion takes place (e.g. in the case of fractal or disordered substrate) [23].

The presence of A/G-GP hydrogel both in the hydrated and lyophilized state influenced the FD-20 release and reduced its mobility compared to PBS by increasing the density and the structural complexity of the material/medium in which FD-20 was entrapped. In fact, in FB-2-H and FB-2-LH samples, the diffusion of FD-20 is mediated by the presence of the hydrogel in different forms. Compared to PBS, the addition of FD-20 into lyophilized hydrogels allowed a longer release even after an initial FD-20 burst release. The use of FD-20 pre-loaded hydrogels (FB-2-H) allowed to significantly reduce the burst release and to maintain a prolonged release (until 168h).

3.4 Feasibility and morphological evaluation of multifunctional nerve guidance channel

Fig. 9 shows the SEM micrograph and μCT images of the fabricated nerve guide composed of a PCL tube containing A/G_GP hydrogel and aligned hollow glass fibres. The fibres were homogeneously dispersed into the guide lumen. The presence of the fibres creates an anisotropic structure mimicking the peripheral nerve topography.

Furthermore, the presence of the hydrogel inside and outside the fibres allows the incorporation of neurotrophic factors, which would be released after implantation. Neurotrophic factor are released from the tube ending site guaranteeing to immediately reach the two nerve stumps avoiding risk of factor denaturation or leakage. The developed device combines both topographical and chemical factors acting as directional cues that are known to enhance the axon regeneration [29]. Moreover, the different strategy of fibres filling described in this work would allow to tailor the release kinetics of the chemical factors reaching a prolonged release with benefits for the regeneration process.

4. CONCLUSIONS

Tailoring the kinetics to achieve a sustained release of growth factors during regeneration process is an important issue in designing scaffolds for tissue regeneration. In a previous work, it was shown that phosphate glass hollow fibres are an effective mean for the incorporation and release of biomolecules [17]. The possibility to tailor the biomolecules release by varying the filling procedures of the glass fibres for FD-20 loading was demonstrated in this work. While the use of a FD-20/PBS solution as fibre filling material resulted in a fast FD-20 release (i.e. about 95% in the first 24 hours), the use of A/G_GP hydrogel as fibre filling material, allowed a slower FD-20 release. In fact, the higher density and structural complexity of the hydrogel is the cause of a reduction of FD-20 mobility compared to PBS. In particular, the fibre filled using FD-20/hydrogel showed a slow release (i.e. complete release after 168 h), while those containing lyophilized hydrogel subsequently filled with FD-20/PBS solution showed an intermediate release rate (i.e. complete release after 72 h).

This novel phosphate glass hollow fibres-A/G_GP hydrogel system can be used to impart both topographical and trophic functionalities to NGC. The fibres create an anisotropic structure inside the NGC which can support the adhesion of glial and neuronal cells and direct the axonal

growth. Moreover, the fibre lumen can be exploited for the incorporation of biomolecules, which can be then released at the tube ends to stimulate and direct the axonal regeneration after injuries.

The mild conditions used for A/G_GP hydrogel preparation guarantees the GFs bioactivity even after encapsulation into the hydrogels. Future works will be performed to load neurotrophic GFs and analyze the release and its effect *in vivo*.

Acknowledgement

BICONERVE project (Regional Project, Regione Piemonte) is acknowledged for co-financing.

Dr. Joris Lousteau (Istituto Superiore Mario Boella, ISMB) and Prof. Daniel Milanese (Politecnico di Torino, DISAT) are acknowledged for the collaboration in the fibre drawing process.

References

1. E.A. Huebner, S.M. Strittmatter, Axon regeneration in the peripheral and central nervous systems, Results Probl Cell Differ 48 (2009) 339-351.

2. B. Battiston, S. Raimondo, P. Tos, V. Gaidano, C. Audisio, A. Scevola, I. Perroteau, S. Geuna, Chapter 11: Tissue engineering of peripheral nerves, Int Rev Neurobiol 87 (2009) 227-249.

3. G. Ronchi, S. Nicolino, S. Raimondo, P. Tos, B. Battiston, I. Papalia, A.S. Varejão, M.G. Giacobini-Robecchi, I. Perroteau, S. Geuna, Functional and morphological assessment of a standardized crush injury of the rat median nerve, J Neurosci Methods 179(1) (2009) 51-57.

4. R. Deumens, A. Bozkurt, M.F. Meek, M.A.E Marcus, E.A.J. Joosten, J. Weis, G. Brook, Repairing injured peripheral nerves: Bridging the gap, Progress in Neurobiology 92 (2010) 245-276.

5. J.S. Belkas, M.S. Shoichet, R. Midha, Axonal Guidance Channels in Peripheral Nerve Regeneration, Oper Tech Orthop 14(3) (2004) 190-198.

6. S. Kehoe, X.F. Zhang, D. Boyd, FDA approved guidance conduits and wraps for peripheral

nerve injury: A review of materials and efficacy, Injury 43(5) (2012) 553-572.

7. M.F. Meek, J.H. Coert, US Food and Drug Administration/Conformit Europe-Approved Absorbable Nerve Conduits for Clinical Repair of Peripheral and Cranial Nerves, ANPS 60(4) (2008) 466-472.

8. A. Pabari, S.Y. Yang, A.M. Seifalian, A. Mosahebi, Modern surgical management of peripheral nerve gap, J Plast Reconstr Aesthet Surg 63 (2010) 1941-1948.

9. W. Daly, L. Yao, D. Zeugolis, A. Windenbank, A. Pandit, A biomaterials approach to peripheral nerve regeneration: bridging the peripheral nerve gap and enhancing functional recovery, J R Soc Interface 9(67) (2012) 202-21.

10. A.C. Lee, V.M. Yu, J.B. Lowe, M.J. Brenner, D.A. Hunter, S.E. Mackinnon, S.E. Sakiyama-Elbert, Controlled release of nerve growth factor enhances sciatic nerve regeneration, Exp Neurol 184 (2003) 295–303.

11. P.G. Cordeiro, B.R. Seckel, S.A. Lipton, P.A. D'Amore, J. Wagner, R. Madison, Acidic fibroblast growth factor enhances peripheral nerve regeneration in vivo, Plast Reconstr Surg 83 (1989) 1013–1019.

12. J.M. Rovak, A.K. Mungara, M.A. Aydin, P.S. Cederna, Effects of Vascular Endothelial Growth Factor on Nerve Regeneration in Acellular Nerve Grafts, J Reconstr Microsurg 20(1) (2004) 53-58.

13. H. Fansa, W. Schneider, G. Wolf, G. Keilhoff, Influence of insulin-like growth factor-I (IGF-I) on nerve autografts and tissue-engineered nerve grafts, Muscle Nerve 26 (2002) 87–93.

14. M.R. Wells, D.K. Batter, H.N. Antoniades, D.G. Blunt, J. Weremowicz, S.E. Lynch, H.A. Hansson, PDGF-BB and IGF-I in combination enhance axonal regeneration in a gap model of peripheral nerve injury, Soc Neurosci Abstr 20 (1994) 1326.

15. K.Y. Lee, M.C. Peters, D.J. Mooney, Comparison of vascular endothelial growth factor and basic fibroblast growth factor on angiogenesis in SCID mice, J Control Release 87 (2003) 49–56.

16. C. Vitale-Brovarone, G. Novajra, J. Lousteau, D. Milanese, S. Raimondo, M. Fornaro, Phosphate glass fibres and their role in neuronal polarization and axonal growth direction, Acta Biomater 8 (2012) 1125–1136.

17. G. Novajra, J. Lousteau, D. Milanese, C. Vitale-Brovarone, Resorbable hollow phosphate glass fibres as controlled release systems for biomedical applications, Materials Letters 99 (2013) 125–127.

18. L.A Pfister, M. Papaloızos, H.P. Merkle, B. Gander, Hydrogel nerve conduits produced from alginate/chitosan complexes, J Biomed Mater Res 80A (2007) 932–37.

19. C. Tonda-Turo, S. Gnavi, F. Ruini, G. Gambarotta, E. Gioffredi, V. Chiono, I. Perroteau, G. Ciardelli, Natural origin injectable hydrogels as filler for peripheral nerve guidance channels, J Tissue Eng Regen Med (2013), submitted.

20. C. Vitale-Brovarone, G. Novajra, D. Milanese, J. Lousteau, J.C. Knowles, Novel phosphate glasses with different amount of TiO_2 for biomedical applications. Dissolution tests and proof of concept of fibre drawing, Mater Sci Eng C 31(2) (2011) 434-442.

21. G. Novajra, C. Vitale-Brovarone, J.C. Knowles, G. Maina, V. Aina, D. Ghigo, L. Bergandi, Effects of TiO_2-containing phosphate glasses on solubility and in vitro biocompatibility, JBMR A 99A (2011) 295-306.

22. C. Audisio, S. Raimondo, S. Nicolino, G. Gambarotta, F. Di Scipio, L. Macrì, F. Montarolo, M.G. Giacobini-Robecchi, P. Porporato, N. Filigheddu, A. Graziani, S. Geuna, I. Perroteau, Morphological and biomolecular characterization of the neonatal olfactory bulb ensheathing cell line, J Neurosci Methods 185(1) (2009) 89–98.

23. V. Papadopoulou, K. Kosmidis, M. Vlachou, P. Macheras, On the use of the Weibull function for the discernment of drug release mechanisms, Int J Pharm. 309(1-2) (2006) 44-50.

24. K. Kosmidis, P. Argyrakis, P. Macheras, A Reappraisal of Drug Release Laws Using Monte Carlo Simulations: The Prevalence of the Weibull Function, Pharmaceuti Res 20(7) (2003) 988-995.

25. C. Tonda-Turo, C. Audisio, S. Gnavi, V. Chiono, P. Gentile, S. Raimondo, S. Geuna, I. Perroteau, G. Ciardelli, Porous Poly(ε-caprolactone) Nerve Guide Filled with Porous Gelatin Matrix for Nerve Tissue Engineering, Adv Eng Mat 13(5) (2011) B151–B164.

26. H. Gao, T. Tan, D. Wang, Dissolution mechanism and release kinetics of phosphate controlled release glasses in aqueous medium, J Control Release 96 (2004) 29-36.

27. Y. Hong, X. Chen, X. Jing, H. Fan, Z. Gu, X. Zhang, Fabrication and Drug Delivery of Ultrathin Mesoporous Bioactive Glass Hollow Fibers, Adv Funct Mater 20 (2010) 1–8.

28. J. Siepmann, N.A. Peppas, Modeling of drug release from delivery systems based on hydroxypropyl methylcellulose (HPMC), Adv Drug Deliver Rev 48 (2011) 139-157.

29. V. Chiono, C. Tonda-Turo, G. Ciardelli, Artificial scaffolds for peripheral nerve reconstruction, Int Rev Neurobiol 87 (2009) 173-199.

Figure captions

Fig. **1.** Weight loss percentage (%WL) of the fibre samples (FB, 2 cm) soaked in culture medium at a (solution volume)/(fibre exposed surface) ratio of 1 ml/cm^2 and stored at 37°C in a humidified atmosphere of 5% CO_2/air (mean value± standard deviation).

Fig. **2.** Cell counts (mean value ± standard error of the mean) obtained for NOBEC cells incubated with “fresh” medium (ctrl), 14 days “aged” medium (ctrl14) and the medium containing the fibre dissolution products after 14 days of dissolution (14F).

Fig. **3.** Results of Western blot analysis after incubation of NOBEC cells with “fresh” medium (ctrl), 28 days “aged” medium (ctrl28) and the medium containing the fibre dissolution products

after 28 days of incubation (28F).

Fig. **4.** Optical micrographs showing hollow fibres filled with a) FD-20/PBS solution (FA-2 samples), b) FD-20-containing hydrogel (FB-2-H samples) and c) lyophilized hydrogel before and d) after filling with FD-20/PBS solution (FB-2-LH samples).

Fig. **5.** FD-20 release percentage (mean value ± standard deviation) from fibres filled with a FD-20/PBS solution (10 mg/ml). Samples: FA fibres (D_{fi} 69 µm) of 2 cm (FA-2), FB fibres (D_{fi} 94 µm) of 1.5 cm (FB-1.5), 2 cm (FB-2) and 2.5 cm (FB-2.5).

Fig. **6.** FD-20 release percentage (mean value ± standard deviation) from FB fibres (D_{fi} 94 µm) of 2 cm filled with FD-20/PBS solution (FB-2), FD-20-containing hydrogel (FB-2-H) and with lyophilized hydrogel and FD-20/PBS solution (FB-2-LH).

Fig. **7.** Regression curves obtained with the interpolation of the release data a) with equation 8 (first 60% of the release curve) derived from the semi-empirical power law (equation 6) and b) with equation 9 (entire release data), derived from the Weibull function (equation 7).

Fig. **8.** Representation of *n* versus *b* parameter estimated for each type of samples. Dotted line is the linear regression curve (*b*= *1.489n+0.0516*) calculated by P apadopoulou *et al.* [23] from the estimated values of *n* and *b* for several experimental and published drug release data.

Fig. **9** Nerve guide composed of a PLC tube containing alignes hollow glass fibers filled with A/G GP hydrogel a) SEM micrograph (transverse section). X-ray absorption microtomography images b) of a transversal section c) of the entire guide in a threedimensional view and d) of the aligned hollow fibers contained into the guide lumen.

Figure 1

Click here to download high resolution image

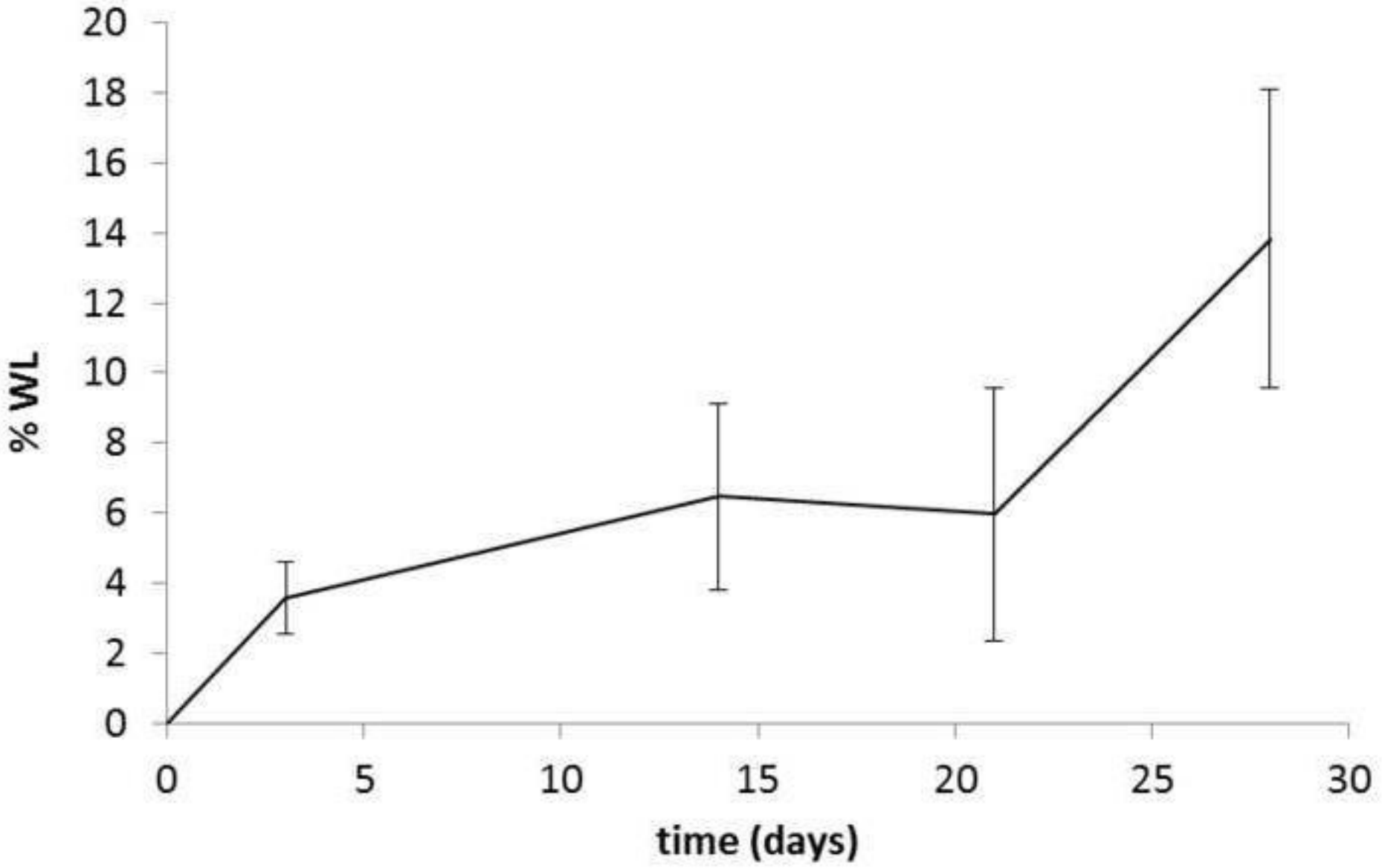

Figure 2

Click here to download high resolution image

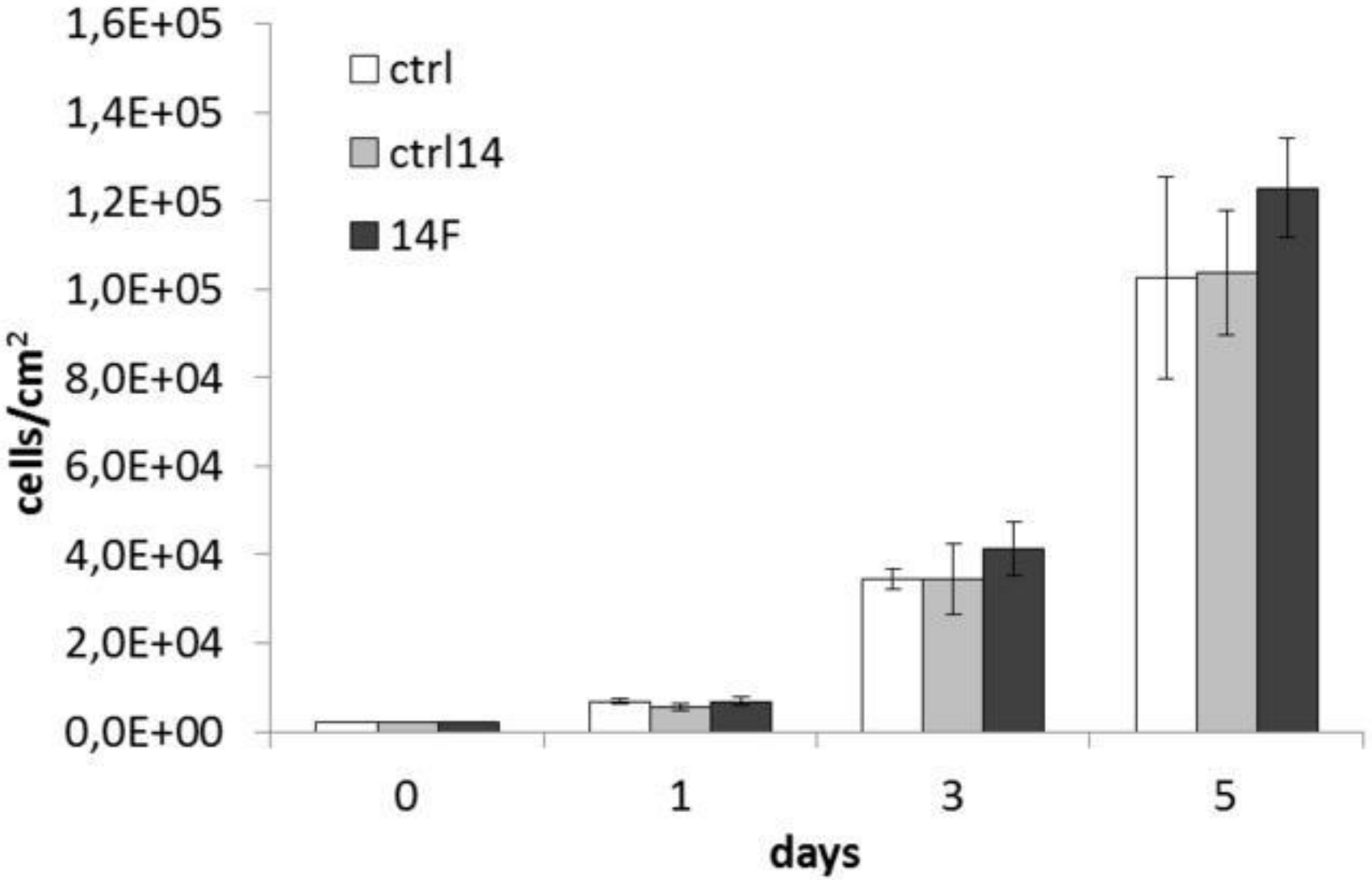

Figure 3

Click here to download high resolution image

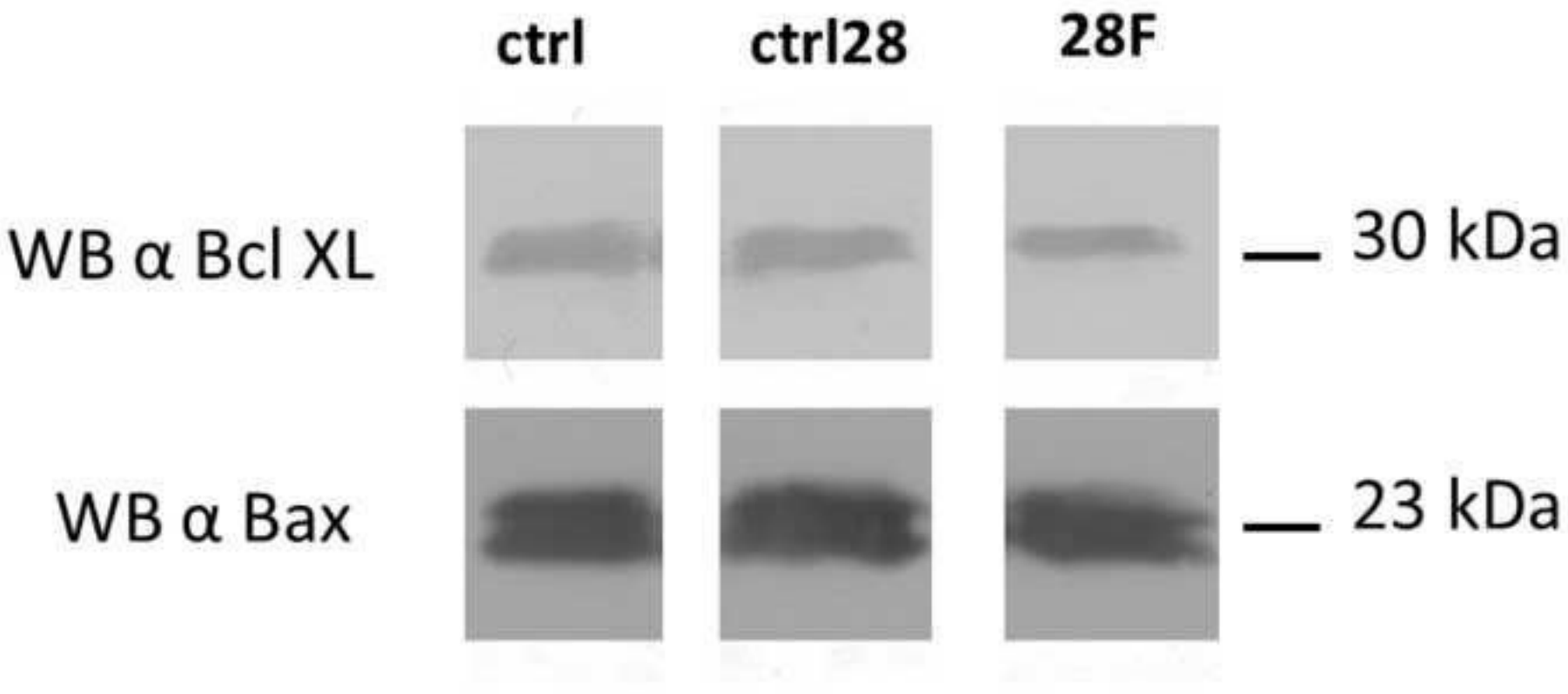

Figure 4

Click here to download high resolution image

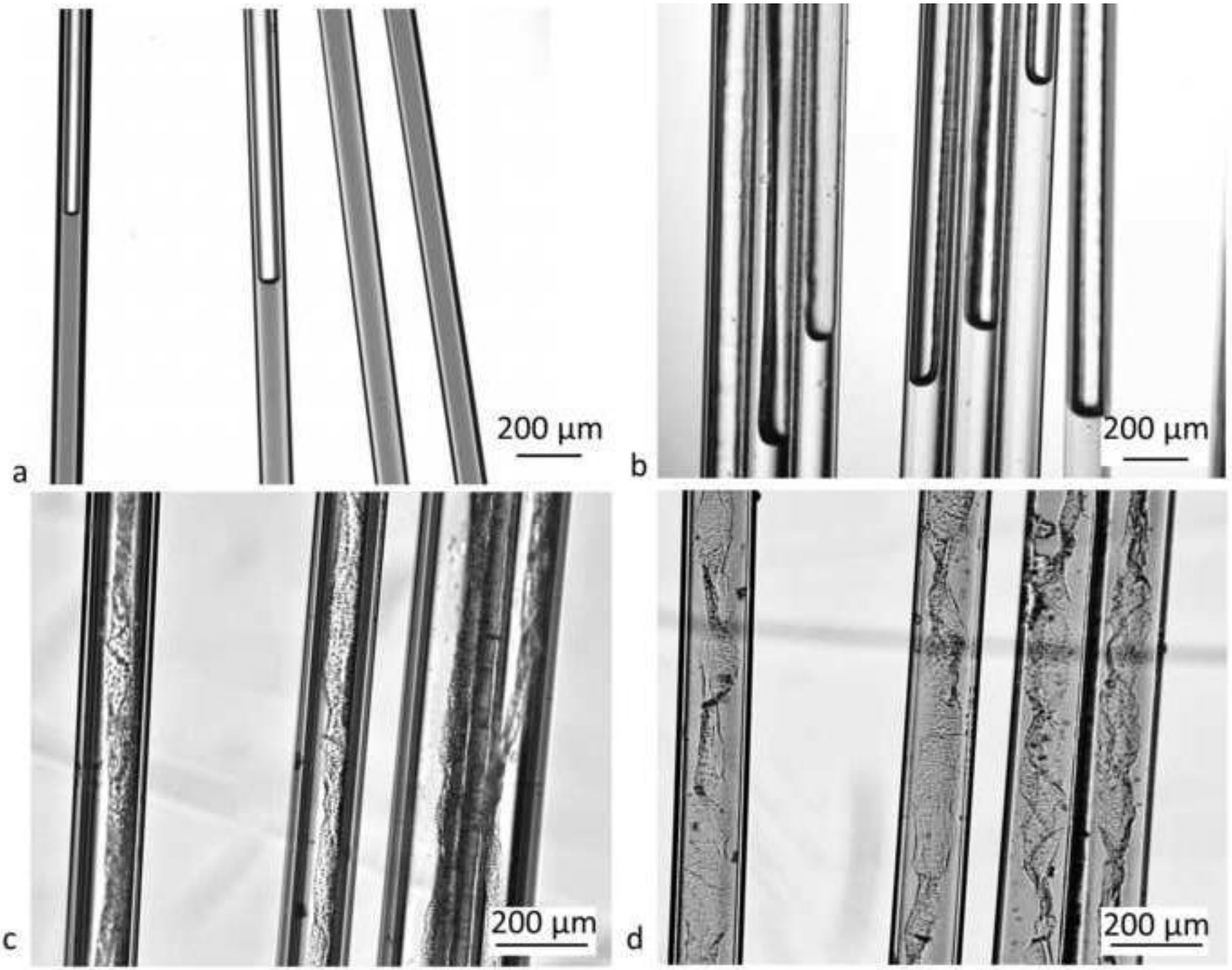

Figure 5

Click here to download high resolution image

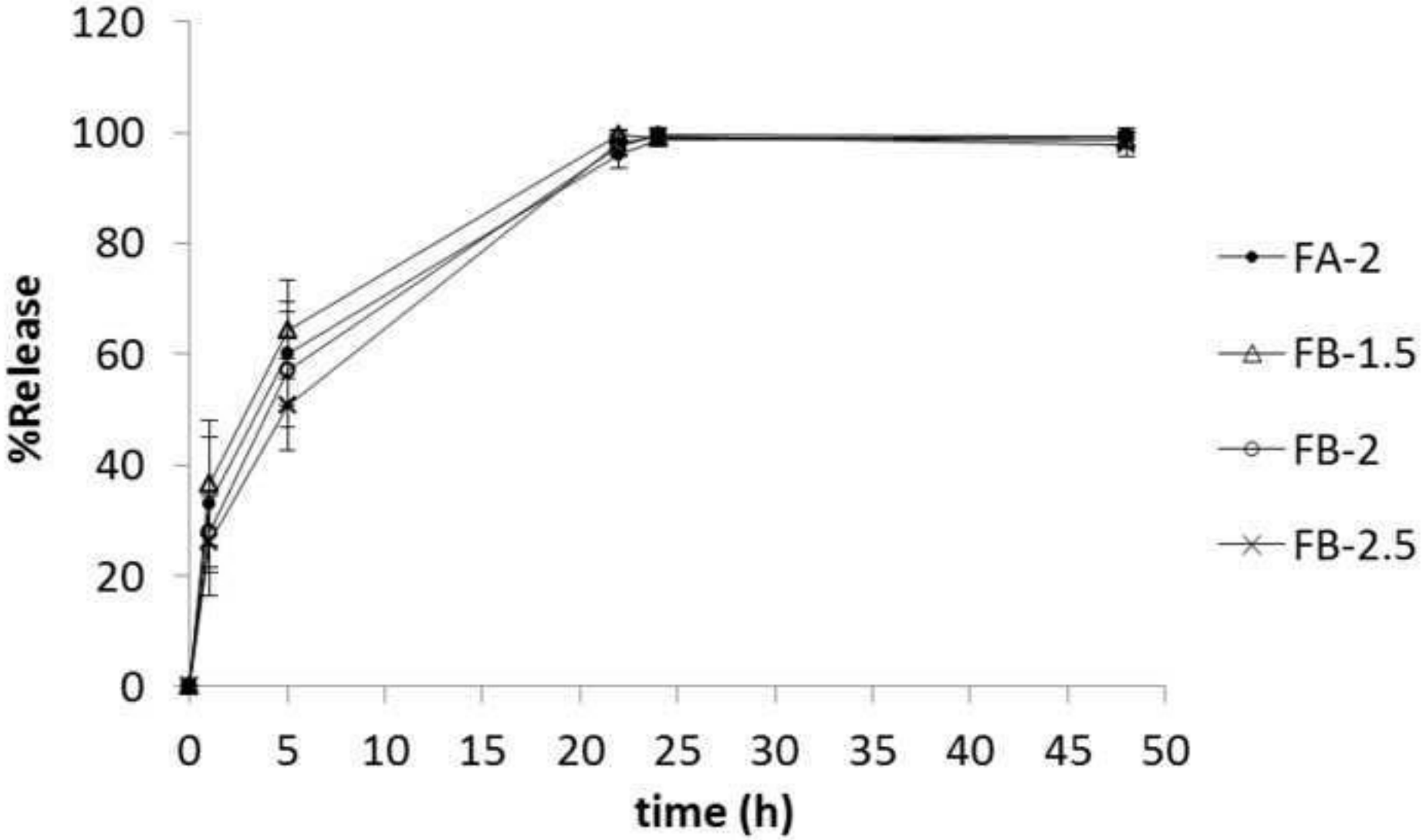

Figure 6

Click here to download high resolution image

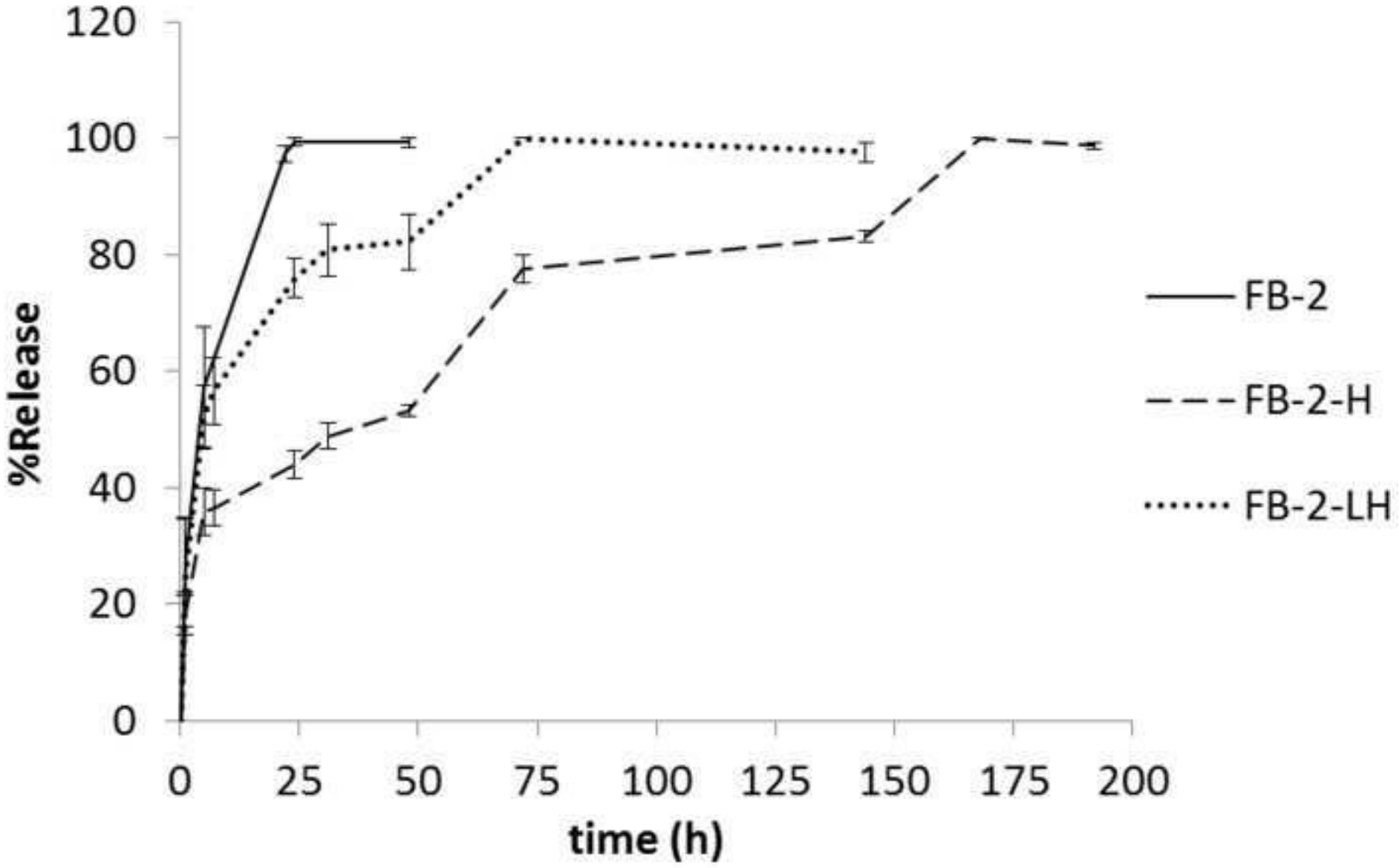

Figure 7

Click here to download high resolution image

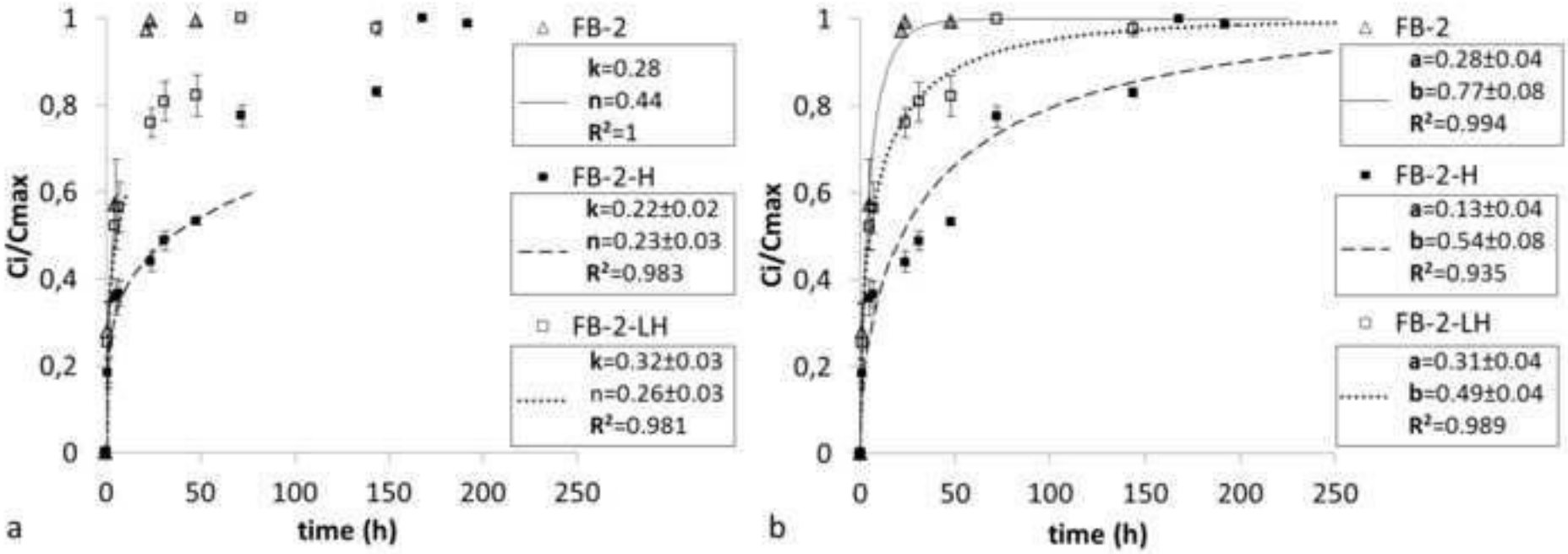

Figure 8

Click here to download high resolution image

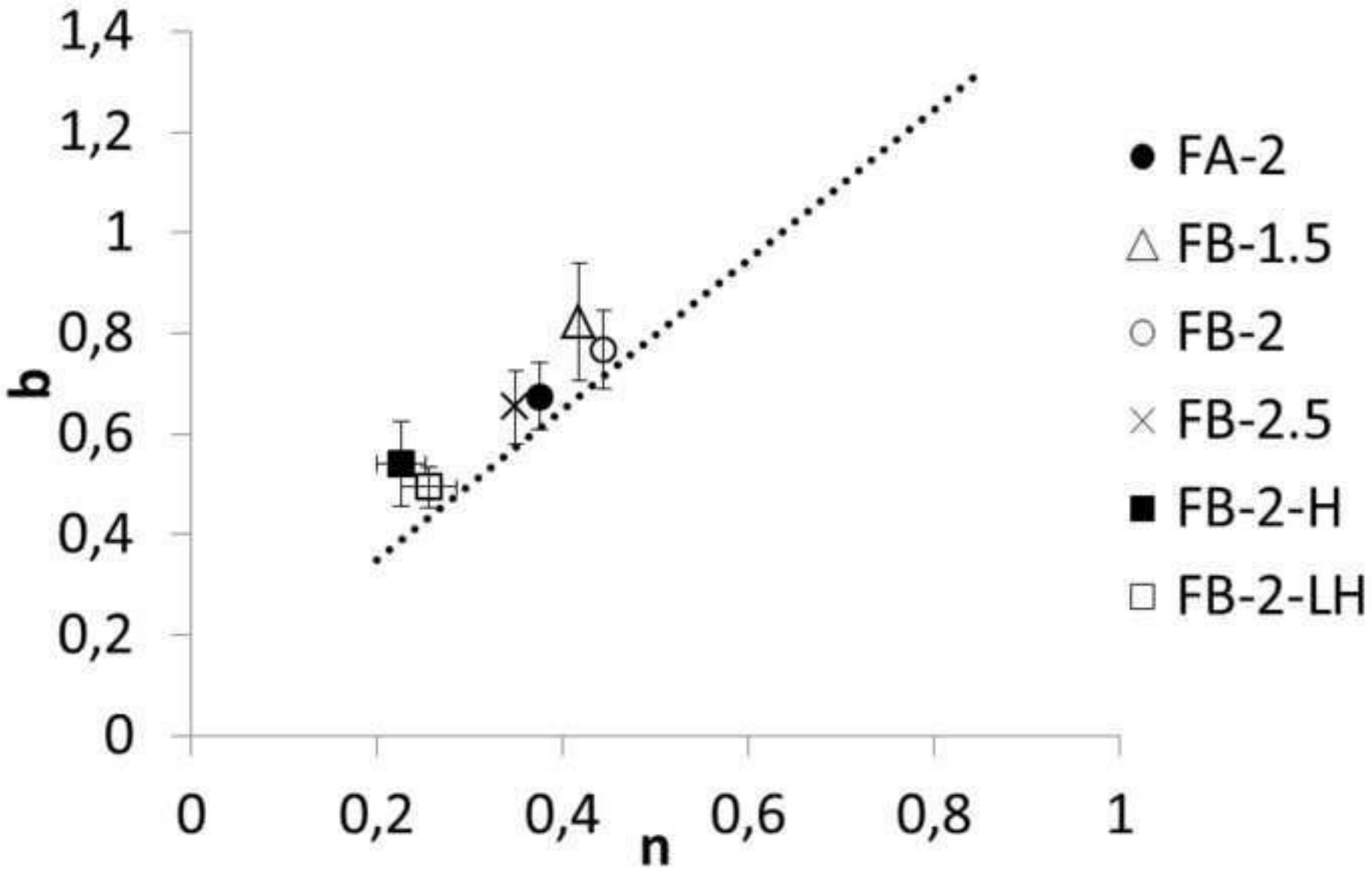

Figure 9

Click here to download high resolution image

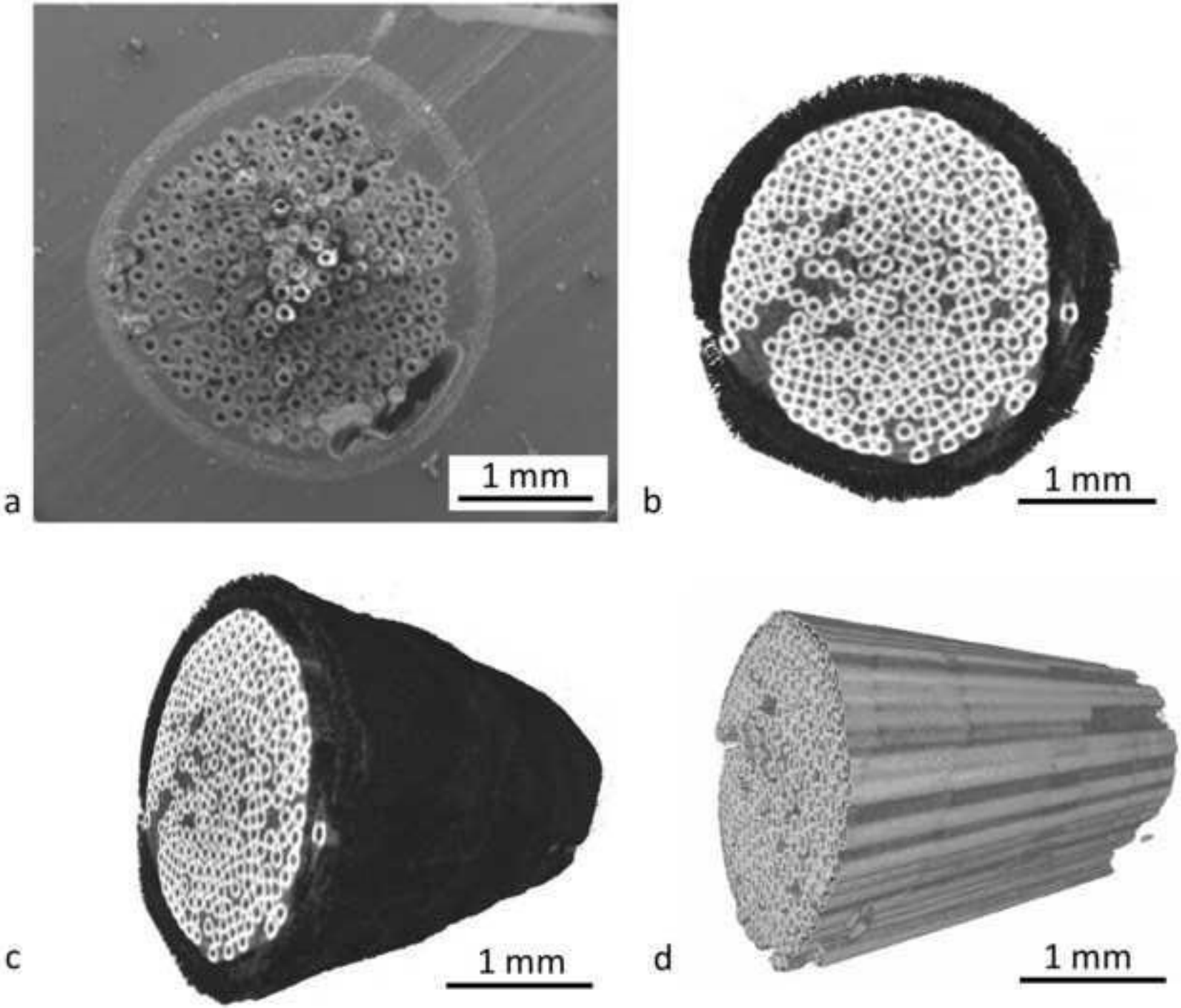

Tables

Table 1. Preform feeding speed (v_p) and fibre speed (v_f) used for fibre drawing with the corresponding theoretical inner (TD_{fi}) and outer (TD_{fo}) diameters of the fibres.

Fibre code	V_p (mm/min)	V_f (m/min)	TD_{fi} (µm)	TD_{fo} (µm)
FA	0.3	2.5	71	124
FB	0.5	2.5	92	160

Table 2. Samples used for the FD-20 release study from the glass hollow fibres

Sample code	Fibre type	Fibre length (cm)	Fibre filler
FA-2	FA	2	FD-20/PBS solution
FB-1.5	FB	1.5	
FB-2		2	
FB-2.5		2.5	
FB-2-H	FB	2	A/G_GP/FD-20
FB-2-LH	FB	2	Lyophilized A/G_GP + FD-20/PBS solution

Table 3. Measured inner and outer diameters (D_{fi}, D_{fo}) of the obtained fibres compared to the theoretical ones (TD_{fi}, TD_{fo})

	Theoretical diameters (µm)		Measured diameters (µm)	
Fibre code	TD_{fi}	TD_{fo}	D_{fi}	D_{fo}
FA	71	124	69 ± 5	121 ± 4
FB	92	160	94 ± 3	167 ± 4